

t-t* Elastic Scattering from 1.6 to 2.0 Mev

DALE M. HOLM AND H. V. ARGO

Los Alamos Scientific Laboratory, University of California, Los Alamos, New Mexico

(Received December 1, 1955)

A magnetically analyzed triton beam from an electrostatic accelerator has been scattered from tritium in a 14-inch scattering chamber and the differential cross section for elastic scattering measured in 10° steps from 20° to 140° in the center-of-mass system for incident energies of 1.8 and 2.0 Mev. Two proportional counters with a fixed angular separation of 90° were used in coincidence to detect both the scattered and recoil tritons for the laboratory range from 45° to 70° , with an absolute probable error of $\pm 3\%$. A single counter was used for laboratory angles between 10° and 20° , with resultant probable errors of $+5\%$, -15% . Excitation functions in 100-kev steps from 1.6 to 2.0 Mev show no evidence for an excited state of He^6 in this region.

INTRODUCTION

ELASTIC scattering measurements for low-energy, low- Z particles will remain of continuing interest to the theoretician as long as the theory of nuclear forces is incomplete. Angular yield information which permits the analysis of the scattering probability in terms of outgoing waves of various angular momenta is particularly useful. Tritium provides an interesting extension to the light-particle scattering experiments. Being a rare isotope of hydrogen, it has only recently become available in sufficient quantities for *t-t* measurements.

The techniques for measuring charged-particle elastic scattering have been highly developed by a number of careful workers.¹⁻³ The most precise measurements have been made using gas targets contained in large scattering chambers, where the incident beam of particles was highly collimated and the particles scattered from a well-defined volume of target were accepted by a high-resolution counter analyzer. An important possible source of error is the presence of high- Z gas contaminants such as air or oil molecules. Another troublesome source of error arises from edge scattering by the defining apertures. Measurements of *t-t* scattering are further complicated by the presence of alpha particles and neutrons covering a continuous energy interval up to several Mev. These particles arise from the various modes of breakup of the compound nucleus, He^6 .

With like-particle scattering, e.g., tritons scattered from tritons, it is possible⁴ to take advantage of the fact that for nonrelativistic energies the recoil nucleus and the scattered particle must always travel at 90° to each other in the laboratory system. With two counters separated by 90° in the laboratory system and arranged to record coincidence counts, one is able to sort out those events that are due to like-particle scattering.

* This work performed under the auspices of the U. S. Atomic Energy Commission.

¹ Tuve, Heydenburg, and Hafstad, Phys. Rev. **50**, 806 (1936).

² Herb, Kerst, Parkinson, and Plain, Phys. Rev. **55**, 998 (1939).

³ Worthington, McGruer, and Findley, Phys. Rev. **90**, 899 (1953).

⁴ R. R. Wilson and E. C. Creutz, Phys. Rev. **71**, 339 (1947).

SCATTERING CHAMBER

The chamber first described by Sherr *et al.*⁵ has been modified considerably. Figures 1 and 2 show the important features and dimensions of the chamber as modified. The beam entered through the collimator at the left in Fig. 1, traversed the scattering chamber, and then was collected by the Faraday cup at the right. The scattered beam particles and corresponding recoil target nuclei were detected by two gas-filled proportional counters mounted on the periphery of a circular plate. A fixed angle of 90° separated the two counters. The circular plate was graduated in 1° intervals about its circumference, and together with the counters was fastened to one end of a movable cone. An O-ring formed a rotary vacuum seal for the cone while six springs provided a spring loading opposite that due to the atmosphere. Rotation of the cone was accomplished by a gear fastened to the bottom of the cone, and the angle of rotation was indicated to one-twentieth of a degree by a fixed vernier scale located at the edge of the graduated circular plate holding the two counters.

The tritium target gas was evolved fresh from a uranium furnace at the start of each day's run. Pressures of about 3 mm Hg as indicated by an oil manometer were used in the chamber. The target gas was confined to the chamber by entrance and exit windows. The entrance windows were of Pyrex glass and had stopping powers in the range 8 to 26 kev for 1-Mev protons. These thin glass windows have been described elsewhere.⁶ Their low stopping power was of great importance here since beam scattering at the entrance foil can result in a serious loss of beam intensity at the chamber center. The exit window was of aluminum foil, thin enough to pass the triton beam but thick enough to stop of $\frac{1}{3}$ -energy protons present in the magnetically analyzed mass-three beam. A 3.1-mg/cm² foil satisfied these requirements for incident beam energies varying from 1.6 Mev to 2.0 Mev.

The beam collimator at the entrance to the chamber consisted of two apertures 0.152 cm in diameter and

⁵ Sherr, Blair, Kratz, Bailey, and Taschek, Phys. Rev. **72**, 662 (1947).

⁶ Arthur Hemmendinger and Arno P. Roensch, Rev. Sci. Instr. **26**, 562 (1955).

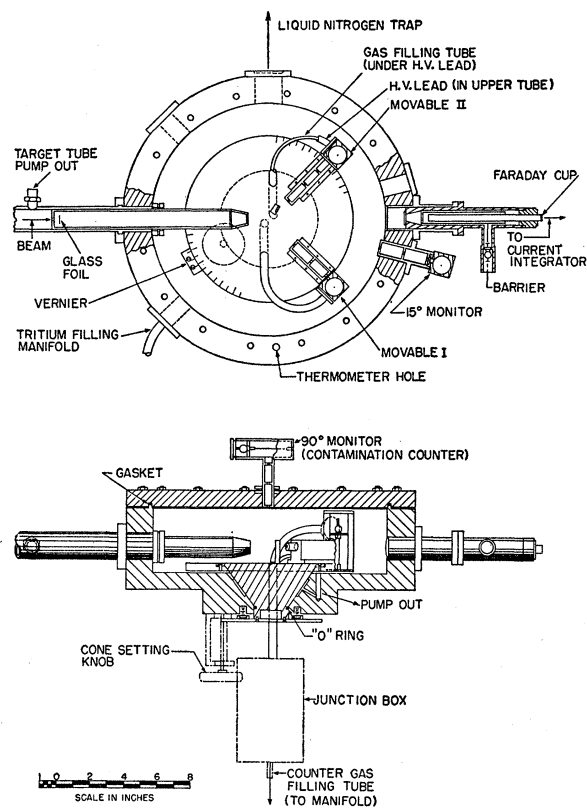


Fig. 1. Plan drawings of scattering chamber.

29.2 cm apart. A third aperture 0.183 cm in diameter and located 2.5 cm beyond the second defining aperture served as a beam "scraper," removing beam particles scattered by preceding aperture edges. The thin glass entrance window was located between the two defining apertures, 0.5 cm from the first one.

In addition to the two movable counters, there were two fixed monitor counters that were useful in monitoring the growth of contaminant gases in the chamber. One of these was in the chamber lid at 90° to the beam, and the other was in the chamber wall at +15° to the beam.

All four gas counters were of similar design. The cylinder was 1 inch in inside diameter and 2.50 inches long. The central wire was made of 3-mil stainless steel. Particles entered the counters perpendicular to the wire along an axis $\frac{1}{8}$ inch from the wire. Two hypodermic needles covered all but the middle 1-inch section of the wire. The counters were filled with a mixture of 2% CO₂ and pure argon to a pressure of about 20 cm Hg. The voltages applied to the wires varied between 700 and 900 volts. To minimize the possible introduction of coincidence counts by the power supply, Movable I counter was supplied by a battery pack.

The counter windows were mounted on the ends of the counter analyzers, as shown in Fig. 3. The window thickness depended upon the function of the counter.

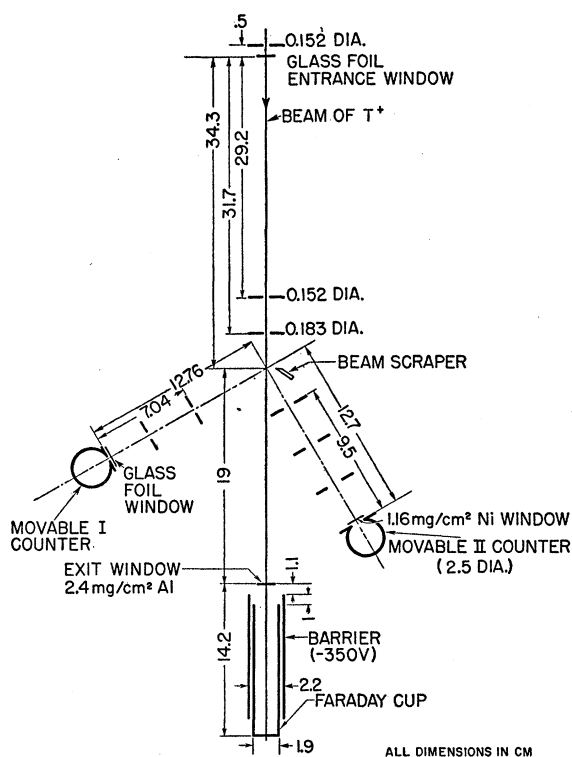


Fig. 2. Schematic drawing showing positions and sizes of the beam collimating apertures and the positions of the counter analyzer apertures.

Movable I counter was the primary detector of the scattered tritons, while Movable II served to verify the counts in Movable I by providing a coincidence count from the corresponding recoil triton. A thin glass window on Movable I permitted the low-energy scattered tritons at angles approaching 90° to be counted, while a 1.16-mg/cm² nickel foil was thin enough to pass the higher energy tritons into Movable II at the corresponding forward angles. A 2.4-mg/cm² aluminum foil window on the 15° monitor stopped the $\frac{1}{3}$ -energy protons from entering this counter but did pass the higher energy tritons. A 1.16-mg/cm² nickel foil was used on the 90° monitor.

The alignment of the beam collimator and movable counters axes was done by optical methods. A careful examination showed that the axis of the cone intersected the beam axis within 0.002 inch, and was tipped from the vertical by about 2 min of angle. These small discrepancies introduced no significant errors into the target volume calculations. The graduated disk holding the two counters was marked with a dividing head on a milling machine and is believed to be accurate to $\pm 0.01^\circ$.

GEOMETRY

The requirement that Movable II counter see all of the target volume defined by the counter analyzer for Movable I resulted in an inconveniently large foil

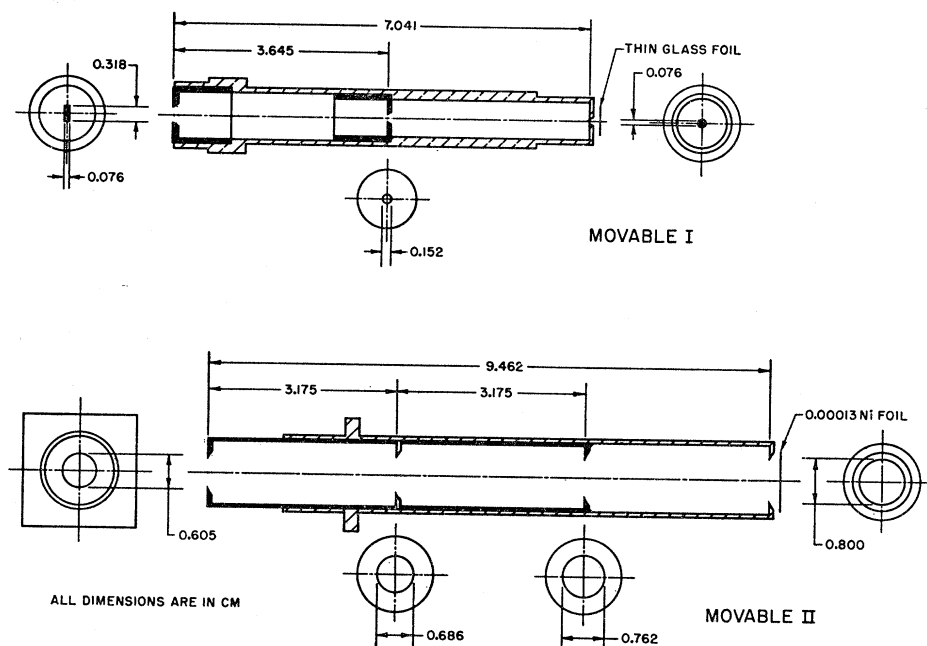


FIG. 3. Movable I and Movable II counter analyzers.

diameter for Movable II. The nature of the problem is illustrated in Fig. 4. Coincidence counting rates as low as 14 counts/min had to be accepted in order that the beam-collimating apertures and Movable I apertures could be made small enough to meet the limitations set by Movable II.

A simplification of the problem results from the fact that for like particles the scattered particle and recoil particle are indistinguishable, and hence the cross section must be perfectly symmetrical about 90° in the c.m. system. For this reason one need measure the yield for only a 45° interval in the laboratory system, 0° to 45° or 45° to 90° . From Fig. 4 it is clear that Movable I counter should be restricted to the angular interval between 45° and 90° in order to keep the size of the entrance aperture of Movable II within bounds. All of the coincidence measurements were taken with Movable I in this interval and Movable II in the corresponding -45° to 0° interval. Hence the maximum apertures for Movable II were required when both counters were at 45° . A single-counter analyzer for Movable II was used and its apertures were set to cover the 45° case.

The counter analyzer for Movable I followed the classical design of Tuve, Heydenburg, and Hafstad.¹ The first defining aperture was rectangular and the second defining aperture was circular. Figure 3 shows the dimensions in detail. One interesting feature of the rectangular slits is that they were removable as a unit. Since the absolute yield is directly proportional to the width of this slit and the dimension involved is very small (0.076 cm), it was important to have the slit edges regular and uniformly spaced. After some experi-

mentation it was found that the commercially available 0.156-inch Starrett round stock was a satisfactory material from which to fashion the slit edges. A relatively simple grinding operation relieved one side of the edge, leaving a slit-edge thickness of 0.003 inch. A small amount of polishing left the slit edges as shown in Fig. 5. Two of these pieces were cut to size and spot-welded to cross members, as shown, the spacing being carefully held while assembling. Calculations showed that a slit-edge thickness of 0.003 inch was ample to stop all protons and tritons of energies below 2 Mev and was thin enough to keep the slit-edge scattering small.

The yield of scattered tritons is given by the following expression:

$$Y = Nn\sigma(\theta)G/\sin\theta, \quad (1)$$

where N is the number of incident tritons, n is the number of target nuclei per unit volume, $\sigma(\theta)$ is the differential scattering cross section at the laboratory angle θ in units of square centimeters per steradian, and G is defined by the usual equation²

$$G = 2b_1A/R_0h, \quad (2)$$

where A is the area of the rear aperture, $2b_1$ is the width of the front slit, h is the distance from the slit to the rear aperture, and R_0 is the distance from the center of the target volume to the rear aperture. For the measurements reported here, G was equal to 3.810×10^{-6} cm.

A knife-edge beam scraper was placed near the target volume as shown in Figs. 1 and 2. It helped to reduce the counting rate of Movable II at the forward angles but did not interfere with this counter's function. The main beam could not hit the scraper at any time.

ELECTRONICS

The output pulses from all four gas counters were amplified and passed through discriminating and scaling circuits in the usual manner. In addition the pulses from the two movable counters were fed into a coincidence circuit with a resolving time of 0.8 μ sec. After a 1- μ sec delay, the signal from Movable I counter was fed into two 18-channel pulse-height analyzers⁷ connected in parallel. One of these analyzers was gated ON for 17 μ sec by a coincidence and the other gated OFF for the same duration. The discriminator thresholds for the two analyzers and the single-scaler unit for Movable I counter were all set equal, so the sum of the counts registered in the two 18-channel analyzers was equal to the counts registered in the single-scaler unit. Thus analyzer number 1 registered the pulses from Movable I that were in coincidence with pulses from Movable II while analyzer number 2 registered those counts in Movable I not accompanied by a coincidence count and therefore due to contaminant scattering or to multiple scattering.

CURRENT MEASUREMENT

During the course of the experiment two different current integrators were used. The first one was used for the data taken at 2.0, 1.9, and 1.8 Mev. The beam charged a small capacitor having low leakage to a preset

value of about 5 volts. An electrometer tube voltmeter measured the voltage and operated a circuit which discharged the capacitor through a mercury relay. A register indicated the number of cycles of the integrator. The integrator was calibrated frequently during each day's run, the current-time method of calibration being employed. The internal consistency of the repeated calibrations was about 0.3%, and the absolute accuracy was 0.5%.

A more reliable current integrator of the Wisconsin type⁸ was used for the lower energy data taken later. A 4- μ f capacitor was charged by battery to -12 volts and discharged by the beam. A vibrating reed electrometer indicated when the charge reached zero. This integrator was calibrated by measurement of the capacitance and the voltage to which it was charged, the over-all accuracy being about 0.2%. An independent calibration using the current time method was made frequently and the two methods always agreed within assigned errors.

Multiple scattering of the triton beam in passing through the aluminum exit foil could cause some of the beam particles to miss the Faraday collection cup. The method of Dickinson and Dodder⁸ for calculating multiple scattering was used to show that for the geometry used here a completely negligible beam loss occurred. A barrier cylinder at a potential of -350 volts prevented secondary electrons from entering or leaving the collector.

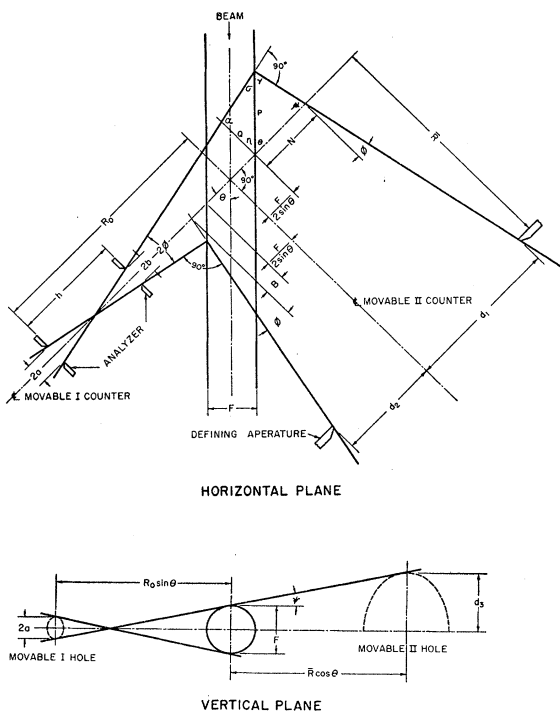


FIG. 4. Entrance aperture requirements for Movable II counter. The angular spread has been exaggerated in the drawings to illustrate clearly the nature of the problem.

⁷ C. W. Johnstone, *Nucleonics* **11**, No. 1, 36 (1953).

EXPERIMENTAL PROCEDURE

The use of 90° coincidence counting introduces a serious problem that is not present in the usual single-counter method of measuring scattering cross sections. The scattered particle always has a finite chance of being scattered a second time by the chamber gas in its path to the detector. The probability of this happening is greater than 1% for the geometry and gas pressure used here. Breit, Thaxton, and Eisenbud⁹ have

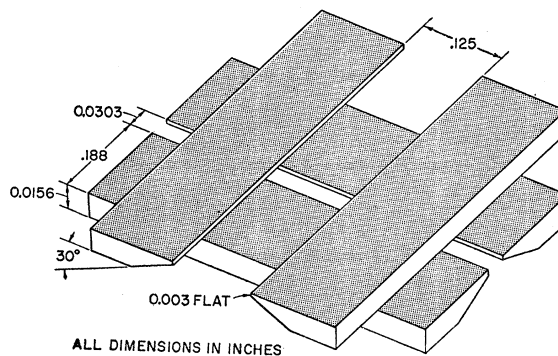


FIG. 5. Pictorial drawing of the slits for the counter analyzers.

⁸ W. C. Dickinson and D. C. Dodder, *Rev. Sci. Instr.* **24**, 428 (1953).

⁹ Breit, Thaxton, and Eisenbud, *Phys. Rev.* **55**, 1018 (1939).

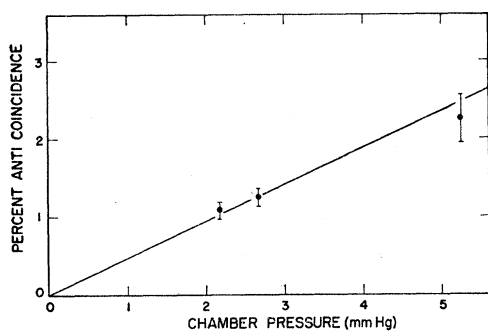


FIG. 6. Secondary gas scattering losses at 45° as a function of the chamber gas pressure.

shown that the effect of this "gas scattering" upon the yield as measured by a single counter is negligible, even when absolute measurements with an accuracy better than 1% are desired. By reason of the symmetry of the geometry, the number of particles lost by gas scattering is almost exactly balanced by the number of particles gained by the same process. The two-counter arrangement used here will not benefit by this fortunate circumstance unless the Movable II counter has a sufficiently large aperture to catch all of the mates of the particles scattered into Movable I by the secondary gas scattering.

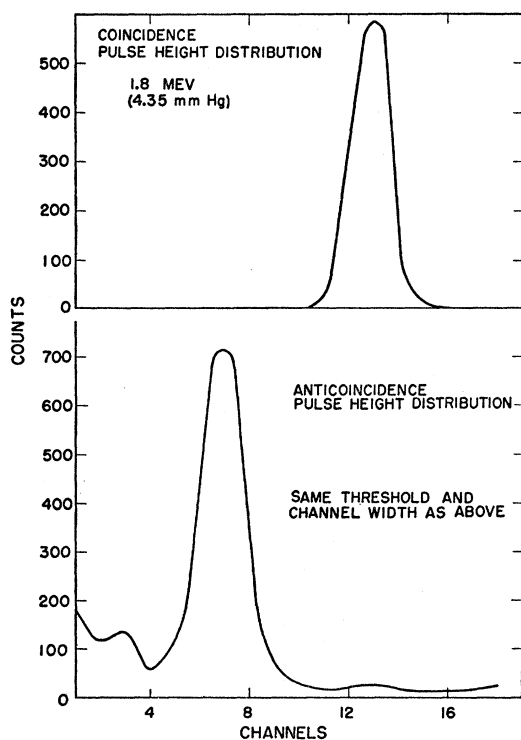


FIG. 7. Representative pulse-height distributions of the counts in Movable I at 45° , separated into coincidence and anticoincidence counts. The anticoincidence distribution contains $p-t$ scattering plus an alpha-particle background

These effects plus the over-all operation of the apparatus were studied by measuring the $p-p$ scattering cross section with the equipment as designed. Since secondary gas scattering is directly proportional to the target gas pressure, its effect could be measured by varying the gas pressure while measuring the yield. With clean hydrogen gas in the chamber and Movable I counter at 45° , all of the counts observed in Movable I fell in a nicely resolved peak when analyzed by pulse height and appeared to be due to $p-p$ scattering. A few of these counts, however, were not recorded in the coincidence analyzer but were shifted to the anticoincidence analyzer, indicating that their recoil mates had not been picked up by Movable II. The ratio of counts recorded in the anticoincidence analyzer to the total number of counts gave the fraction of counts lost due to secondary gas scattering. In Fig. 6 are shown the fractional losses plotted as a function of the target gas pressure for Movable I at 45° . The curve is a straight line, the losses being zero at zero gas pressure. At 3 mm Hg gas pressure, the loss was 1.1%, which is approximately the calculated loss.

The two extremes of the angular interval covered by coincidence counting were 45° and 70° . For laboratory angles greater than 70° the scattered particles had insufficient energy for reliable detection by the counter. There are two factors influencing the amount of the gas scattering losses: the aperture size for Movable II and the energy of the scattered particle. At 45° the losses due to aperture requirements will be a maximum, while at 70° the losses caused by the increased scattering of the lower energy particles will be a maximum. A second series of measurements with Movable I at 70° and various gas pressures showed that the fractional loss by gas scattering was the same as in Fig. 6 for 45° . The intermediate angles were then investigated by holding the chamber gas pressure fixed and varying the angle of Movable I from 70° down to below 45° , measuring the ratios of anticoincidence counts to totals at each position. As expected, the losses decreased slightly in the intermediate positions and then increased rapidly as one moved below the limiting angle of 45° . The gas-scattering corrections to be applied were assigned a generous probable error of about 50%. Since secondary gas-scattering corrections arise almost completely from small-angle Coulombic collisions at these relatively low energies, the above corrections for $p-p$ secondary scattering are equally applicable to $t-t$ scattering.

The effect of aperture edge scattering from the entrance slit of Movable I counter analyzer was checked by replacing the slit system having 0.003-inch flats on the edges with another system having 0.008-inch flats. The counting rate as well as the ratio of anticoincidence to total counts remained unchanged.

As a final check on the over-all operation of the apparatus, the $p-p$ differential cross section at 45° was

measured for incident protons of 1.858-Mev energy. The value obtained was 0.4783 with a probable error of 1.4%. Corrections for gas-scattering losses have been applied. This absolute value is to be compared with the measurements of Worthington *et al.*³ who obtained the value 0.4748 with a 0.3% probable error. Our value is 0.7% high, well within the probable error.

At this point, tritium gas was placed in the target chamber and a triton beam was accelerated into it. Superimposed upon the pulse height peak caused by tritons scattered from tritons into Movable I were many background counts coming from various sources. The magnetically analyzed beam contained both T^+ and HHH^+ ions in an unknown ratio. The chamber gas was principally tritium (85 to 94%), with the remainder being hydrogen and small amounts of oxygen, nitrogen, and oil vapors. The beam nuclei scattered from all of these target nuclei. Another source of background counts was alpha particles from the breakup of the compound nucleus, He^6 , formed in the $T-T$ interaction.

TABLE I. Nonsystematic uncertainties of measurements.

Source	Uncertainty (%)	Remarks
G -factor [see Eq. (2)]	± 0.3	
Height of oil column	± 0.1	
Oil density	± 0.1	
Gas temperature	± 0.1	
Electronic counting losses	Negligible	
Current integration	± 0.5	For 1.8-, 1.9-, and 2.0-Mev data
Current integration	± 0.2	For 1.6- and 1.7-Mev data
Gas concentration	± 0.4	
Secondary gas scattering	± 0.5	

This reaction can go in one of several ways:

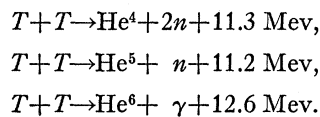


Figure 7 shows the pulse-height distributions of the counts in Movable I when set at 45° . A comparison of the coincidence and anticoincidence distributions shows that the coincidence technique was very effective in separating the background particles from the desired scattered particles. The coincidence counting rate of the order of 14 counts/min set a practical lower limit of 2% for statistical errors.

The angular range beyond 70° was covered in a somewhat crude manner by placing Movable I at the complementary angles, i.e., less than 20° , and using it without coincidence discrimination against the background. Data were taken at the small angles only when fresh gas was in the chamber. For these angles the background corrections were necessarily high and poorly known and the assigned probable errors reflect the lack of knowledge of the background corrections.

TABLE II. Center-of-mass *t-t* elastic scattering cross sections for incident triton energies of 2.013, 1.890, and 1.800 Mev.^a

Triton energy (Mev)	$\phi_{c.m.}$	$\sigma(\phi)_{c.m.}$ (barns/sterad)	Uncertainties (%)	
			Statistical	Total
2.013	30°	0.41	...	± 15
	40°	0.159	...	+5, -15
	130°	0.1103 ^b	± 3.0	± 3.1
	110°	0.0815 ^b	± 3.7	± 3.8
	100°	0.0881 ^b	± 4.0	± 4.1
1.890	90°	0.0795 ^b	± 2.0	± 2.2
	30°	0.43	...	± 15
	120°	0.948 ^b	± 2.7	± 2.8
1.800	90°	0.0787 ^b	± 2.0	± 2.2
	20°	2.90	...	+5, -15
	30°	0.60	...	± 15
	40°	0.197	...	+5, -15
	140°	0.1790 ^b	± 2.3	± 2.5
	50°	0.136	...	+5, -15
	130°	0.1161 ^b	± 2.0	± 2.2
	60°	0.096	...	+5, -15
	120°	0.1007 ^b	± 2.3	± 2.5
	110°	0.0891 ^b	± 2.0	± 2.2
	100°	0.0831 ^b	± 2.1	± 2.3
90°	0.0824 ^b	± 2.6	± 2.8	

^a Probable error due to measurements are 0.8% (see Table I).

^b Measurement made using the 90° coincidence technique.

^c Due to symmetry about 90° in the c.m. system, these two bracketed angles should have the same observed $\sigma(\phi)$.

MEASUREMENTS

Angular Measurements.—The 0° setting of the protractor was confirmed by making yield measurements with Movable I for small angles on both sides of zero. The very rapid increase in yield near 0° made this a sensitive check and the two yield curves (plus and minus angles) were identical within statistical errors, indicating that indeed the 0° axis passed through the 0° setting of the protractor.

Gas Concentration.—Liquid nitrogen trapping helped to remove the contaminant gases but did not eliminate them. Samples of the target gas were taken at the beginning and end of each day's run and were analyzed on a Consolidated-Nier mass spectrometer. The tritium concentration varied from 94.1% to 86.3%. The rate of growth of contamination as given by the 15° monitor counter agreed well with the growth as measured by

TABLE III. Center-of-mass *t-t* elastic scattering cross sections for incident energies of 1.687 and 1.582 Mev.^a

Triton energy (Mev)	$\phi_{c.m.}$	$\sigma(\phi)_{c.m.}$ (barns/sterad)	Uncertainties (%)	
			Statistical	Total
1.687	30°	0.478	...	+5, -15
	60°	0.100	...	+5, -15
	90°	0.0904 ^b	± 3.0	± 3.1
1.582	30°	0.59	...	± 15
	40°	0.261	...	+5, -15
	50°	0.136	...	+5, -15
	60°	0.119	...	+5, -15
	110°	0.1042 ^b	± 3.0	± 3.1
	80°	0.088	...	+5, -15
	90°	0.0959 ^b	± 2.7	± 2.8

^a Probable error due to measurements are 0.8% (see Table I).

^b Measurement made using the 90° coincidence technique.

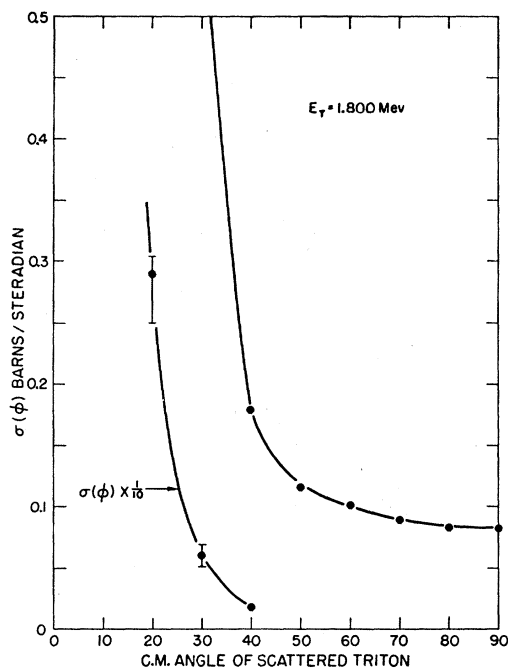


FIG. 8. Angular distribution in the c.m. system for $E_t = 1.800$ Mev.

the gas analysis. The tritium concentration as measured is believed to have an over-all probable error of $\pm 0.4\%$.

Beam Energy.—The machine energy was calibrated in the usual way by measuring the $T^3(p,n)He^3$ threshold using a zirconium-tritium target.¹⁰ The chamber entrance window was then inserted and, with a small amount of helium gas in the chamber to provide cooling for the window, the $T^3(p,n)He^3$ threshold was remeasured. A typical measurement gave an energy loss in the window of about 10 kev and 2 kev in the cooling gas. The change of stopping power with energy for protons in glass was assumed to be the same as for protons in aluminum over the energy range of interest here (500 kev to 1 Mev) and the corresponding energy losses of the triton beam in the window were calculated. In this way the triton energy at the center of the chamber was known to 3 kev.

Pressure.—Tritium pressure in the scattering chamber was measured by means of an oil manometer containing Narcoil-20 oil. The heights of the oil columns were compared with a Wild precision cathetometer located 20 inches from the manometer. The column heights could be measured with an accuracy of 0.005 cm and the resulting uncertainty was 0.1% or less. The density of the oil as a function of temperature was known to 0.1%.¹¹

Temperatures.—Both uniformity and stability of temperatures in the chamber were assured by the good thermal conductivity and large mass of the aluminum

¹⁰ Taschek, Argo, Hemmendinger, and Jarvis, Phys. Rev. **76**, 325 (1949).

¹¹ A. Hemmendinger and H. V. Argo, Phys. Rev. **98**, 70 (1955).

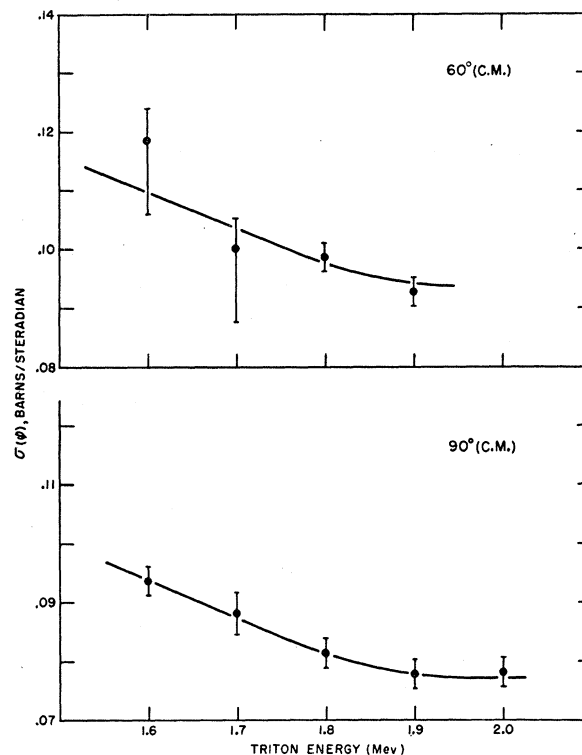


FIG. 9. Excitation functions at c.m. angles of 60° and 90° .

chamber. The temperature of the chamber was measured by a mercury-glass thermometer graduated in tenths of a degree and placed in a well in the wall. The temperature of the manometer oil was indicated by a similar thermometer immersed in the oil of one arm of the manometer.

G-factor [Eq. (2)].—Aperture dimensions were measured by means of a microcomparator and were accurate to 0.1%. The lengths h and $R_0 - h$ were measured with micrometers calibrated immediately before measurement was made. The distances were known to 0.0007 inch and the resulting accuracy was better than 0.05%. A conservative estimate of the accuracy of the G -factor is 0.3%.

SUMMARY OF ERRORS

Table I lists all of the known significant sources of error and the uncertainties that have been assigned to each.

RESULTS

Final values of the differential scattering cross sections are listed in Tables II and III in the c.m. system. Figure 8 shows some of these data plotted in the form of an angular distribution. The total probable errors for the points are listed in the tables and are indicated on the curves. The values labeled with a superscript b were taken with the coincidence counters and one notes that their probable errors are considerably smaller than are the probable errors for the

